

This is an Open Access document downloaded from ORCA, Cardiff University's institutional repository: <https://orca.cardiff.ac.uk/id/eprint/109774/>

This is the author's version of a work that was submitted to / accepted for publication.

Citation for final published version:

Zhao, Yan, Li, Yuyin, Zhang, Yahui and Kennedy, David 2018. Nonstationary seismic response analysis of long-span structures by frequency domain method considering wave passage effect. *Soil Dynamics and Earthquake Engineering* 109 , pp. 1-9. 10.1016/j.soildyn.2018.02.029

Publishers page: <http://dx.doi.org/10.1016/j.soildyn.2018.02.029>

Please note:

Changes made as a result of publishing processes such as copy-editing, formatting and page numbers may not be reflected in this version. For the definitive version of this publication, please refer to the published source. You are advised to consult the publisher's version if you wish to cite this paper.

This version is being made available in accordance with publisher policies. See <http://orca.cf.ac.uk/policies.html> for usage policies. Copyright and moral rights for publications made available in ORCA are retained by the copyright holders.



Nonstationary Seismic Response Analysis of Long-span Structures by Frequency Domain Method Considering Wave Passage Effect

Yan Zhao^a, Yuyin Li^a, Yahui Zhang^{a*}, David Kennedy^b

^a State Key Laboratory of Structural Analysis for Industrial Equipment, Department of Engineering Mechanics, International Center for Computational Mechanics, Dalian University of Technology, Dalian 116023, PR China;

^b School of Engineering, Cardiff University, Cardiff CF24 3AA, Wales, UK

Corresponding author:

Dr. Y. H. Zhang

State Key Laboratory of Structural Analysis for Industrial Equipment, Department of Engineering Mechanics, Dalian University of Technology, Dalian 116023, PR China

Email: zhangyh@dlut.edu.cn

Tel: +86 411 84706337

Fax: +86 411 84708393

1 **Abstract**

2 In this paper, a frequency domain method is proposed for the nonstationary seismic
3 analysis of long-span structures subjected to random ground motions considering the
4 wave passage effect. Based on the correlation analysis theory and fast Fourier transform
5 (FFT), a semi-analytical solution is derived for the evolutionary power spectral density
6 of the random response of long-span structures in the frequency domain. The expression
7 of this solution indicates that the evolutionary property of nonstationary random
8 responses can be determined completely by the modulation function of random ground
9 motions, and hence the solution has clear physical interpretations. For slowly varying
10 modulation functions, the FFT can be implemented with a small sampling frequency, so
11 the present method is very efficient within a given accuracy. In numerical examples,
12 nonstationary random responses of a long-span cable stayed bridge to random ground
13 motions with the wave passage effect are studied by the present method, and comparisons
14 are made with those of the pseudo excitation method (PEM) to verify the present method.
15 Then the accuracy and efficiency of the present method with different sampling
16 frequencies are compared and discussed. Finally, the influences of the apparent velocity
17 of the seismic waves on nonstationary random responses are investigated.

18 **Key words:** seismic analysis; wave passage effect; nonstationary; evolutionary power
19 spectral density; frequency domain method

20 **1 Introduction**

21 During an earthquake, the energy released at the epicenter transfers to the ground
22 surface in the form of seismic waves. Since the waves travel along different paths and
23 through a complex medium, ground motions caused by the earthquake at different
24 locations will have significant differences. Even if the propagation medium is exactly
25 uniform, there is still a difference in the arrival times of seismic waves at different
26 locations due to their different distances to the epicenter. This phenomenon is known as
27 the “wave passage effect”. Long-span structures are generally important facilities, e.g.
28 long-span bridges, dams, or nuclear power plants. Therefore, their aseismatic capabilities
29 are highly relevant to public safety. In seismic analysis, long-span structures have their
30 own special features compared to general building structures. A major feature is that these
31 structures extend over long distances parallel to the ground, so their supports undergo
32 different motions during an earthquake. Hence, the dynamic behaviors of long-span
33 structures with and without consideration of the wave passage effect have significant
34 differences [1, 2].

35 The time-history method is widely applied for the random analysis of long-span
36 structures subjected to an earthquake with spatial variation [3]. This method is based on
37 stochastic simulation, and response parameters (mainly mean values and variances) are
38 obtained through statistical analysis of samples of the random responses. Its main
39 drawback, however, is that it has a huge computational cost. Over three decades, some

40 more efficient methods have been developed. One of them is an extension of the
41 conventional response spectrum method, which was initially only feasible for uniform
42 seismic excitation. Der Kiureghian and Neuenhofer [4] developed a special response
43 spectrum method for the response of structures to a random earthquake considering the
44 wave passage effect, incoherence effect and site-response effect. Yamamura and Tanaka
45 [5] presented an analysis of a suspension bridge to multi-support seismic excitations. In
46 their work, ground motions within a group of adjacent supports on continuous soil or rock
47 were assumed to be uniform and synchronized, while those of different groups were
48 treated as non-uniform and uncorrelated. Berrah and Kausel [6] proposed a modified
49 response spectrum method to address the problem of long-span structures subjected to
50 imperfectly correlated seismic excitations. However, they did not consider the influence
51 of quasi-static displacement. Due to the naturally random properties of the earthquake, it
52 is more rational to study the seismic response of long-span structures using random
53 vibration theory. Heredia-Zavoni and Vanmarcke [7] developed a random vibration
54 method for the seismic analysis of linear multi-support systems. This method reduced the
55 response evaluation to that of a series of linear one degree systems in a way that fully
56 accounts for the space-time correlation structure of the ground motion. Lee and Penzien
57 [8] studied random responses of piping systems under multi-support excitations,
58 obtaining mean and extreme values of the systems in either the time or the frequency
59 domain. Lin et al. [9] simplified a surface-mounted pipeline as an infinitely long

60 Bernoulli-Euler beam attached to evenly spaced ground supports, and solved its random
61 seismic responses. Zanardo et al. [10] carried out a parametric study of the pounding
62 phenomenon associated with the seismic response of multi-span simply supported bridges
63 with base isolation devices. Tubino et al. [11] investigated the influence of the partial
64 correlation of the seismic ground motion on long-span structures by introducing suitable
65 equivalent spectra. Lupoi et al. [12] studied the effects of the spatial variation of ground
66 motion on the response of bridge structures. The results showed that the spatial variation
67 affects the random response considerably. Lin et al. [13-14] proposed a random vibration
68 method known as the pseudo-excitation method (PEM). In the framework of the PEM,
69 the random vibration analysis was reduced to relatively simple harmonic or transient
70 analysis, and hence its computation was of high efficiency. The PEM was also used for
71 seismic responses of long-span structures to ground motion with spatial variations.

72 In the research mentioned above, ground motions were always assumed to be
73 stationary random processes. However, some practical observation results showed that
74 the intensity of the ground motion had three obvious stages, i.e. increasing, steady and
75 decreasing, during the duration of the earthquake. Hence it is more rational to assume the
76 ground motion as a nonstationary random process. Spectral methods, such as Wigner-
77 Ville spectrum [15], physical spectrum [16], evolutionary spectrum [17,18] etc., can
78 provide a general description of the energy-frequency properties of nonstationary
79 processes, and thus have been a focal point of study. The evolutionary power spectral

80 density (PSD) was widely used in the earthquake engineering for its clear physical
81 interpretation and relatively simple mathematical derivation [19,20]. An evolutionary
82 PSD is always defined as the product of a deterministic uniform or nonuniform
83 modulation function and a stationary PSD. Based on a spectral representation based
84 simulation algorithm, Deodatis [21] introduced an iterative scheme to generate seismic
85 ground motion samples at several locations on the ground surface that were compatible
86 with prescribed response spectra, correlated according to a given coherence function,
87 include the wave passage effect. Alderucci and Muscolino [22] presented a random
88 vibration analysis of linear classically damped structural systems subjected to fully
89 nonstationary multicorrelated excitations and gave a closed-form solution of the
90 evolutionary PSD of the response. Combining the experimental data of a multi-support
91 seismic shaking table test and structural health monitoring findings, Ozer et al. [23]
92 developed a framework to evaluate random seismic response and estimate reliability of
93 bridges under multi-support excitations. In the authors' previous works [13,24], the PEM
94 and a highly accurate step-by-step integration method named the Precise Integration
95 Method (PIM) were combined to solve nonstationary random responses of long-span
96 structures under the earthquake with consideration of the wave passage effect. Generally,
97 a time-frequency domain analysis is required to obtain the solution of the evolutionary
98 PSD when structures are excited by a nonstationary random excitation. During the time-
99 frequency domain analysis, the time domain integration is performed at each frequency

100 point. To achieve accurate results, small time steps are required in the time domain
101 integration, especially for a wide band random excitation with high frequency
102 components. Hence, there will inevitably be a huge computational cost.

103 Combining the evolutionary PSD and correlation analysis theory, this paper
104 develops a frequency domain method for the random vibration analysis of long-span
105 structures subjected to ground motions with the wave passage effect. This method can be
106 used to obtain the semi-analytical solution of the evolutionary PSD of random responses
107 and its computation is very efficient. This paper is structured as follows. In section 2,
108 governing equations of long-span structures subjected to nonuniform earthquake
109 excitation are given. Section 3 presents the evolutionary PSD model with consideration
110 of the wave passage effect. By separating the deterministic modulation function from the
111 evolutionary PSD, section 4 establishes a frequency domain method to obtain the semi-
112 analytical solution of random responses. In section 5, a long-span cable-stayed bridge is
113 adopted as an example structure. The present method is applied to random vibration
114 analysis of the bridge and the results are compared to those of the PEM to verify the
115 present method. The influences of the wave velocity on random responses are compared
116 and discussed. Section 6 gives some conclusions.

117 **2 Governing equations of structures under nonuniform seismic** 118 **excitation**

119 The governing equations of a long-span structure with N supports and n degrees

120 of freedom (DOF) subjected to nonuniform seismic excitation can be written as [25]

121

$$\begin{bmatrix} \mathbf{M}_{aa} & \mathbf{M}_{ab} \\ \mathbf{M}_{ab}^T & \mathbf{M}_{bb} \end{bmatrix} \begin{Bmatrix} \ddot{\mathbf{y}}_a(t) \\ \ddot{\mathbf{y}}_b(t) \end{Bmatrix} + \begin{bmatrix} \mathbf{C}_{aa} & \mathbf{C}_{ab} \\ \mathbf{C}_{ab}^T & \mathbf{C}_{bb} \end{bmatrix} \begin{Bmatrix} \dot{\mathbf{y}}_a(t) \\ \dot{\mathbf{y}}_b(t) \end{Bmatrix} + \begin{bmatrix} \mathbf{K}_{aa} & \mathbf{K}_{ab} \\ \mathbf{K}_{ab}^T & \mathbf{K}_{bb} \end{bmatrix} \begin{Bmatrix} \mathbf{y}_a(t) \\ \mathbf{y}_b(t) \end{Bmatrix} = \begin{Bmatrix} \mathbf{0} \\ \mathbf{p}_b(t) \end{Bmatrix} \quad (1)$$

122

123 where the subscripts ‘‘a’’ and ‘‘b’’ indicate the non-support and support DOF, respectively;

124 $\mathbf{y}_a(t)$ is an n -dimensional vector containing all non-support displacements; m -

125 dimensional vectors $\mathbf{y}_b(t)$ and $\mathbf{p}_b(t)$ represent the enforced support displacements and

126 forces at all supports, respectively; the $n \times n$ matrices \mathbf{M}_{aa} , \mathbf{C}_{aa} and \mathbf{K}_{aa} [\mathbf{M}_{bb} , \mathbf{C}_{bb}

127 and \mathbf{K}_{bb}] are the mass, damping and stiffness matrices associated with $\mathbf{y}_a(t)$ [$\mathbf{y}_b(t)$];

128 the superscript ‘‘T’’ denotes transposition. Note that when the lumped mass matrix

129 approximation is adopted, \mathbf{M}_{ab} is null.

130 In order to solve Eq. (1), the absolute displacement $\mathbf{y}_a(t)$ can be decomposed into

131 the following two parts [25]:

132

$$\begin{Bmatrix} \mathbf{y}_a(t) \\ \mathbf{y}_b(t) \end{Bmatrix} = \begin{Bmatrix} \mathbf{y}_s(t) \\ \mathbf{y}_b(t) \end{Bmatrix} + \begin{Bmatrix} \mathbf{y}_d(t) \\ \mathbf{0} \end{Bmatrix} \quad (2)$$

133

134 in which $\mathbf{y}_s(t)$ and $\mathbf{y}_d(t)$ are the quasi-static and dynamic displacement vectors,

135 respectively, which satisfy the following equations:

136

$$\begin{bmatrix} \mathbf{K}_{aa} & \mathbf{K}_{ab} \\ \mathbf{K}_{ab}^T & \mathbf{K}_{bb} \end{bmatrix} \begin{Bmatrix} \mathbf{y}_s(t) \\ \mathbf{y}_b(t) \end{Bmatrix} = \begin{Bmatrix} \mathbf{0} \\ \mathbf{p}_b(t) \end{Bmatrix} \quad (3)$$

137

138 Expanding the first row of Eq. (3) gives

139

$$\mathbf{y}_s(t) = -\mathbf{K}_{aa}^{-1} \mathbf{K}_{ab} \mathbf{y}_b(t) \quad (4)$$

140

141 Assuming that the damping force is proportional to the dynamic relative velocity

142 $\dot{\mathbf{y}}_d(t)$ instead of $\dot{\mathbf{y}}_a(t)$, the first row of Eq. (1) can be rewritten as

143

$$\mathbf{M}_{aa}\ddot{\mathbf{y}}_d(t) + \mathbf{C}_{aa}\dot{\mathbf{y}}_d(t) + \mathbf{K}_{aa}\mathbf{y}_d(t) = \mathbf{M}_{aa}\mathbf{K}_{aa}^{-1}\mathbf{K}_{ab}\ddot{\mathbf{y}}_b(t) \quad (5)$$

144

145 In the random vibration analysis of long-span structures under nonuniform seismic

146 excitation, seismic waves are always assumed to travel along a certain direction. For long-

147 span structures with N supports, the accelerations of ground motions at supports in the

148 travelling direction can be expressed as the following N -dimensional vector

149

$$\ddot{\mathbf{u}}_b(t) = \{\ddot{u}_1(t), \ddot{u}_2(t), \dots, \ddot{u}_N(t)\}^T \quad (6)$$

150

151 At the same time, $\ddot{\mathbf{y}}_b(t)$ in Eq. (5) can also be expressed as the following m -
152 dimensional ground acceleration vector

153

$$\ddot{\mathbf{y}}_b(t) = \{\ddot{y}_1(t), \ddot{y}_2(t), \dots, \ddot{y}_m(t)\}^T \quad (7)$$

154

155 Further, the transformation relation between $\ddot{\mathbf{y}}_b(t)$ and $\ddot{\mathbf{u}}_b(t)$ can be written as

156

$$\ddot{\mathbf{y}}_b(t) = \mathbf{E}_{mN}\ddot{\mathbf{u}}_b(t) \quad (8)$$

157

158 in which \mathbf{E}_{mN} is an $m \times N$ block-diagonal matrix. Obviously, if no rotational

159 components are considered for each support, then $m = 3N$.

160 It is assumed that α is the angle between the horizontal travelling direction of the

161 seismic wave and the x -axis, which is defined as the longitudinal direction of the long

162 structure. Hence for P waves, \mathbf{E}_{mN} can be expressed as

163

$$\begin{bmatrix} \cos\alpha & 0 & \cdots & 0 \\ \sin\alpha & 0 & \cdots & 0 \\ 0 & 0 & \cdots & 0 \\ 0 & \cos\alpha & \cdots & 0 \\ 0 & \sin\alpha & \cdots & 0 \\ 0 & 0 & \cdots & 0 \\ \vdots & \vdots & \ddots & \vdots \\ 0 & 0 & \cdots & \cos\alpha \\ 0 & 0 & \cdots & \sin\alpha \\ 0 & 0 & \cdots & 0 \end{bmatrix} \quad (9)$$

164

165 while for SH and SV waves, each sub-matrix in \mathbf{E}_{mN} becomes $\{-\sin\alpha \ \cos\alpha \ 0\}^T$

166 and $\{0 \ 0 \ 1\}^T$, respectively.

167 According to the transformation relation of Eq. (8), the right-hand term of Eq. (5)

168 can be directly expressed by the ground acceleration at the support. Now, the equation of

169 motion is similar to that of a uniform excitation earthquake, i.e.

170

$$\mathbf{M}_{aa}\ddot{\mathbf{y}}_d(t) + \mathbf{C}_{aa}\dot{\mathbf{y}}_d(t) + \mathbf{K}_{aa}\mathbf{y}_d(t) = \mathbf{R}\ddot{\mathbf{u}}_b(t) \quad (10)$$

171

172 in which

173

$$\mathbf{R} = \mathbf{M}_{aa}\mathbf{K}_{aa}^{-1}\mathbf{K}_{ab}\mathbf{E}_{mN} \quad (11)$$

174

175 **3 Nonstationary random ground motion model with wave**

176 **passage effect**

177 The seismic ground motion is assumed to be a uniformly modulated nonstationary

178 random process which is widely used in earthquake engineering. Considering the wave

179 passage effect, i.e. the difference in the arrival times of waves, the ground accelerations

180 at supports can be written as

181

$$\ddot{\mathbf{u}}_b(t) = \mathbf{G}(t)\ddot{\mathbf{x}}(t) \quad (12)$$

182

183 where

184

$$\mathbf{G}(t) = \text{diag}[g(t - t_1), g(t - t_2), \dots, g(t - t_N)], \quad \ddot{\mathbf{x}}(t) = \begin{Bmatrix} \ddot{x}(t - t_1) \\ \ddot{x}(t - t_2) \\ \vdots \\ \ddot{x}(t - t_N) \end{Bmatrix} \quad (13)$$

185

186 in which $\mathbf{G}(t)$ is a diagonal matrix whose diagonal element $g(t)$ is a slowly varying

187 modulation function and $\ddot{\mathbf{x}}(t)$ is a vector consisting of the stationary random process

188 $\ddot{x}(t)$.

189 According to the Wiener-Khinchin theorem, the auto correlation function

190 $R_{\ddot{x}\ddot{x}}(t_1 - t_2)$ of the stationary random process $\ddot{x}(t)$ can be expressed as

191

$$R_{\ddot{x}\ddot{x}}(t_1 - t_2) = E[\ddot{x}(t_1)\ddot{x}(t_2)] = \int_{-\infty}^{+\infty} S_{\ddot{x}\ddot{x}}(\omega) e^{i\omega(t_1 - t_2)} d\omega \quad (14)$$

192

193 where $S_{\ddot{x}\ddot{x}}(\omega)$ is the auto PSD function of $\ddot{x}(t)$.

194 Since the acceleration $\ddot{x}(t)$ is a stationary random process, the displacement $x(t)$

195 is also stationary. It has been proved [13] that the auto PSDs $S_{\ddot{x}\ddot{x}}(\omega)$ and $S_{xx}(\omega)$ and

196 cross PSDs $S_{x\ddot{x}}(\omega)$ and $S_{\ddot{x}x}(\omega)$ satisfy the relationships

197

$$\begin{aligned} S_{xx}(\omega) &= \frac{1}{\omega^4} S_{\ddot{x}\ddot{x}}(\omega) \\ S_{x\ddot{x}}(\omega) &= S_{\ddot{x}x}(\omega) = -\frac{1}{\omega^2} S_{\ddot{x}\ddot{x}}(\omega) \end{aligned} \quad (15)$$

198

199 **4 Frequency domain method for nonstationary random**
200 **vibration analysis considering wave passage effect**

201 **4.1 Correlation analysis of random response**

202 For a linear structure under the seismic excitation expressed in Eq. (12), the dynamic
203 relative displacement vector can be written in the convolution integral form as follows

204

$$\mathbf{y}_d(t) = \int_{-\infty}^{+\infty} \mathbf{h}(\tau) \mathbf{R} \ddot{\mathbf{u}}_b(t - \tau) d\tau \quad (16)$$

205

206 where $\mathbf{h}(\tau)$ is the impulse response function matrix. $\mathbf{h}(\tau)$ is related to the frequency
207 response function matrix $\mathbf{H}(\omega)$ as a Fourier transform pair, i.e.

208

$$\mathbf{h}(\tau) = \frac{1}{2\pi} \int_{-\infty}^{\infty} \mathbf{H}(\omega) e^{i\omega\tau} d\omega, \quad \mathbf{H}(\omega) = \int_{-\infty}^{\infty} \mathbf{h}(\tau) e^{-i\omega\tau} d\tau \quad (17)$$

209

210 According to Eqs. (4) and (8), the quasi-static displacement \mathbf{y}_s can be expressed as
211

$$\mathbf{y}_s(t) = -\mathbf{M}_{aa}^{-1} \mathbf{R} \mathbf{u}_b(t) \quad (18)$$

212

213 where $\mathbf{u}_b(t)$ is the displacement vector of the supports.

214 Substituting Eqs. (16) and (18) into Eq. (2) gives

215

$$\mathbf{y}_a(t) = \mathbf{y}_d(t) + \mathbf{y}_s(t) = \int_{-\infty}^{+\infty} \mathbf{h}(\tau) \mathbf{R} \ddot{\mathbf{u}}_b(t - \tau) d\tau - \mathbf{M}_{aa}^{-1} \mathbf{R} \mathbf{u}_b(t) \quad (19)$$

216

217 It is noted that the first part of the right hand side of Eq. (19) is equivalent to a
218 dynamic analysis with uniform excitation, while the second part is a linear transformation.

219 For a linear system with nonstationary random excitation, the random responses are also
 220 nonstationary. In order to assess the stochastic characteristics of random responses, a
 221 correlation analysis is performed based on random vibration theory. Multiplying each side
 222 of Eq. (19) by its transposition and performing an ensemble average gives
 223

$$\begin{aligned} E[\mathbf{y}_a(t_k)\mathbf{y}_a^T(t_l)] = & \\ & E[\mathbf{y}_d(t_k)\mathbf{y}_d^T(t_l)] + E[\mathbf{y}_s(t_k)\mathbf{y}_d^T(t_l)] + E[\mathbf{y}_d(t_k)\mathbf{y}_s^T(t_l)] \\ & + E[\mathbf{y}_s(t_k)\mathbf{y}_s^T(t_l)] \end{aligned} \quad (20)$$

224

225 Thus the autocorrelation function of the absolute displacement response $\mathbf{y}_a(t)$
 226 consists of four parts which are the autocorrelation functions and cross-correlation
 227 functions of the dynamic relative displacement response $\mathbf{y}_d(t)$ and the quasi-static
 228 displacement response $\mathbf{y}_s(t)$.

229 In order to facilitate the derivation, the autocorrelation function of the dynamic
 230 relative displacement response $\mathbf{y}_d(t)$, i.e. the first term on the right hand side of Eq. (20),
 231 is studied first, and can be expressed as

232

$$\begin{aligned} E[\mathbf{y}_d(t_k)\mathbf{y}_d^T(t_l)] &= \int_{-\infty}^{+\infty} \int_{-\infty}^{+\infty} \mathbf{h}(\tau_k)\mathbf{R}(E[\ddot{\mathbf{u}}_b(t_k - \tau_k)\ddot{\mathbf{u}}_b^T(t_l - \tau_l)])\mathbf{R}^T\mathbf{h}^T(\tau_l)d\tau_kd\tau_l \\ &= \int_{-\infty}^{+\infty} \int_{-\infty}^{+\infty} \mathbf{h}(\tau_k)\mathbf{R}\mathbf{G}(t_k - \tau_k)(E[\ddot{\mathbf{x}}(t_k - \tau_k)\ddot{\mathbf{x}}^T(t_l - \tau_l)]) \\ & \quad \mathbf{G}^T(t_l - \tau_l)\mathbf{R}^T\mathbf{h}^T(\tau_l)d\tau_kd\tau_l \end{aligned} \quad (21)$$

233

234 Thus the autocorrelation function of $\mathbf{y}_d(t)$ is related to the autocorrelation function
 235 of the stationary random acceleration vector $\ddot{\mathbf{x}}(t)$. To further simplify the results, setting
 236 $\bar{t}_k = t_k - \tau_k$ and $\bar{t}_l = t_l - \tau_l$ and applying the relation expressed in Eq. (14) gives

237

$$\begin{aligned}
& E[\ddot{\mathbf{x}}(t_k - \tau_k)\ddot{\mathbf{x}}^T(t_l - \tau_l)] = E[\ddot{\mathbf{x}}(\bar{t}_k)\ddot{\mathbf{x}}^T(\bar{t}_l)] \\
& = \begin{bmatrix} E[\ddot{x}(\bar{t}_k - t_1)\ddot{x}(\bar{t}_l - t_1)] & E[\ddot{x}(\bar{t}_k - t_1)\ddot{x}(\bar{t}_l - t_2)] \cdots E[\ddot{x}(\bar{t}_k - t_1)\ddot{x}(\bar{t}_l - t_n)] \\ E[\ddot{x}(\bar{t}_k - t_2)\ddot{x}(\bar{t}_l - t_1)] & E[\ddot{x}(\bar{t}_k - t_2)\ddot{x}(\bar{t}_l - t_2)] \cdots E[\ddot{x}(\bar{t}_k - t_2)\ddot{x}(\bar{t}_l - t_n)] \\ \vdots & \vdots & \ddots & \vdots \\ E[\ddot{x}(\bar{t}_k - t_n)\ddot{x}(\bar{t}_l - t_1)] & E[\ddot{x}(\bar{t}_k - t_n)\ddot{x}(\bar{t}_l - t_2)] \cdots E[\ddot{x}(\bar{t}_k - t_n)\ddot{x}(\bar{t}_l - t_n)] \end{bmatrix} \quad (22) \\
& = \int_{-\infty}^{\infty} \begin{bmatrix} 1 & e^{i\omega(t_1-t_2)} & \cdots & e^{i\omega(t_1-t_n)} \\ e^{i\omega(t_2-t_1)} & 1 & \cdots & e^{i\omega(t_2-t_n)} \\ \vdots & \vdots & \ddots & \vdots \\ e^{i\omega(t_n-t_1)} & e^{i\omega(t_n-t_2)} & \cdots & 1 \end{bmatrix} e^{i\omega(\bar{t}_k-\bar{t}_l)} S_{\ddot{x}\ddot{x}}(\omega) d\omega \\
& = \int_{-\infty}^{\infty} \mathbf{W}^* \mathbf{e} \mathbf{e}^T \mathbf{W}^T e^{i\omega(\bar{t}_k-\bar{t}_l)} S_{\ddot{x}\ddot{x}}(\omega) d\omega
\end{aligned}$$

239

240 where

241

$$\mathbf{W} = \text{diag}[e^{-i\omega t_1}, e^{-i\omega t_2}, \dots, e^{-i\omega t_N}], \quad \mathbf{e} = \begin{Bmatrix} 1 \\ 1 \\ \vdots \\ 1 \end{Bmatrix} \quad (23)$$

242

243 Substituting Eq. (22) into Eq. (21), the auto correlation function of $\mathbf{y}_d(t)$ can be

244 further expressed as

245

$$E[\mathbf{y}_d(t_k)\mathbf{y}_d^T(t_l)] = \int_{-\infty}^{+\infty} \boldsymbol{\alpha}_d^*(t_k, \omega) \boldsymbol{\alpha}_d^T(t_l, \omega) d\omega \quad (24)$$

246

247 where

248

$$\begin{aligned}
\boldsymbol{\alpha}_d(t, \omega) &= \int_{-\infty}^{+\infty} \mathbf{h}(\tau) \ddot{\mathbf{x}}(t - \tau, \omega) d\tau \\
\ddot{\mathbf{x}}(t, \omega) &= \mathbf{G}(t) \mathbf{W} \mathbf{e} \sqrt{S_{\ddot{x}\ddot{x}}(\omega)} e^{i\omega t}
\end{aligned} \quad (25)$$

249

250 The remaining three terms on the right hand side of Eq. (20) can be dealt in a similar

251 way. For simplicity, their final expressions are given directly as follows:

252 (1) the auto correlation function of quasi - static displacement response $\mathbf{y}_s(t)$ can

253 be expressed as

254

$$\begin{aligned} E[\mathbf{y}_s(t_k)\mathbf{y}_s^T(t_l)] &= \int_{-\infty}^{+\infty} \boldsymbol{\alpha}_s^*(t_k, \omega)\boldsymbol{\alpha}_s^T(t_l, \omega)d\omega \\ \boldsymbol{\alpha}_s(t, \omega) &= -\mathbf{M}_{aa}^{-1}\mathbf{R}\tilde{\mathbf{x}} \\ \tilde{\mathbf{x}}(t, \omega) &= \mathbf{G}(t)\mathbf{W}\mathbf{e}\sqrt{S_{xx}(\omega)}e^{i\omega t} = \frac{1}{\omega^2}\mathbf{G}(t)\mathbf{W}\mathbf{e}\sqrt{S_{\ddot{x}\ddot{x}}(\omega)}e^{i\omega t} \end{aligned} \quad (26)$$

255

256 (2) the cross correlation function of dynamic relative displacement response $\mathbf{y}_d(t)$

257 and quasi - static displacement response $\mathbf{y}_s(t)$ can be expressed as

258

$$E[\mathbf{y}_d(t_k)\mathbf{y}_s^T(t_l)] = \int_{-\infty}^{+\infty} \boldsymbol{\alpha}_d^*(t_k, \omega)\boldsymbol{\alpha}_s^T(t_l, \omega)d\omega \quad (27)$$

259

260 (3) the cross correlation function of quasi - static displacement response $\mathbf{y}_s(t)$ and

261 dynamic relative displacement response $\mathbf{y}_d(t)$ can be expressed as

262

$$E[\mathbf{y}_s(t_k)\mathbf{y}_d^T(t_l)] = \int_{-\infty}^{+\infty} \boldsymbol{\alpha}_s^*(t_k, \omega)\boldsymbol{\alpha}_d^T(t_l, \omega)d\omega \quad (28)$$

263

264 Using Eqs. (24) - (28) and setting $t_k = t_l = t$, the auto correlation function of the

265 absolute displacement response $\mathbf{y}_a(t)$ can be expressed as

266

$$E[\mathbf{y}_a(t)\mathbf{y}_a^T(t)] = \int_{-\infty}^{+\infty} (\boldsymbol{\alpha}_d(t, \omega) + \boldsymbol{\alpha}_s(t, \omega))^*(\boldsymbol{\alpha}_d(t, \omega) + \boldsymbol{\alpha}_s(t, \omega))^T d\omega \quad (29)$$

267

268 According to the Wiener-Khinchin theorem, the integrand function on the right hand

269 side of Eq. (29) is simply the PSD function of the absolute displacement response $\mathbf{y}_a(t)$,

270 which is

271

$$\mathbf{S}_{y_a y_a}(t, \omega) = (\boldsymbol{\alpha}_d(t, \omega) + \boldsymbol{\alpha}_s(t, \omega))^* (\boldsymbol{\alpha}_d(t, \omega) + \boldsymbol{\alpha}_s(t, \omega))^T \quad (30)$$

272

273 Then the time-dependent variance of absolute displacement response $\mathbf{y}_a(t)$ can be

274 obtained as

275

$$\sigma^2(t) = 2 \int_0^\infty \mathbf{S}_{y_a y_a}(t, \omega) d\omega \quad (31)$$

276

277 **4.2 Frequency domain method for evolutionary PSD analysis**

278 In the evolutionary PSD analysis of random responses of long-span structures, the

279 dynamic relative displacement response $\mathbf{y}_d(t)$ is always calculated by using time

280 domain methods. Hence, a small time step should be selected to achieve accurate results

281 when high frequency components are involved in the excitation. However, the small time

282 step makes the calculation inefficient. To solve this situation, a frequency domain method

283 is presented for nonstationary vibration analysis of long-span structures. This method

284 separates the deterministic and random vibration analyses and provides a semi-analytical

285 solution for random responses with clear physical interpretations.

286 Applying the Fourier transform to $\ddot{\mathbf{x}}(t, \omega)$ in Eq. (25) gives

287

$$\begin{aligned} \ddot{\mathbf{X}}(\tilde{\omega}, \omega) &= \int_{-\infty}^{+\infty} \ddot{\mathbf{x}}(t, \omega) e^{-i\tilde{\omega}t} dt = \int_{-\infty}^{+\infty} (\mathbf{G}(t)\mathbf{W}(\omega)\mathbf{e}\sqrt{S_{\ddot{x}\ddot{x}}(\omega)}e^{i\omega t}) e^{-i\tilde{\omega}t} dt \\ &= \tilde{\mathbf{G}}(\tilde{\omega} - \omega)\mathbf{W}(\omega)\mathbf{e}\sqrt{S_{\ddot{x}\ddot{x}}(\omega)} \end{aligned} \quad (32)$$

288

289 where ω should be considered as a constant. The inverse transform of Eq. (32) can be

290 expressed as

291

$$\begin{aligned}\ddot{\mathbf{x}}(t, \omega) &= \frac{1}{2\pi} \int_{-\infty}^{+\infty} \ddot{\mathbf{X}}(\tilde{\omega}, \omega) e^{i\tilde{\omega}t} d\tilde{\omega} \\ &= \frac{1}{2\pi} \int_{-\infty}^{+\infty} \tilde{\mathbf{G}}(\tilde{\omega} - \omega) \mathbf{W}(\omega) \mathbf{e} \sqrt{S_{\ddot{x}\ddot{x}}(\omega)} e^{i\tilde{\omega}t} d\tilde{\omega}\end{aligned}\quad (33)$$

292

293 where $\tilde{\mathbf{G}}(\tilde{\omega})$ is the Fourier transform matrix of $\mathbf{G}(t)$ and can be written as

294

$$\tilde{\mathbf{G}}(\tilde{\omega}) = \int_{-\infty}^{+\infty} \mathbf{G}(t) e^{-i\tilde{\omega}t} dt \quad (34)$$

295

296 Combining Eq. (32) and (33), $\alpha_d(t, \omega)$ in Eq. (24) can be expressed as

297

$$\alpha_d(t, \omega) = \beta_d(t, \omega) \sqrt{S_{\ddot{x}\ddot{x}}(\omega)} e^{i\omega t} \quad (35)$$

298

299 where

300

$$\beta_d(t, \omega) = \left(\frac{1}{2\pi} \int_{-\infty}^{+\infty} \mathbf{H}(\tilde{\omega} + \omega) \tilde{\mathbf{G}}(\tilde{\omega}) e^{i\tilde{\omega}t} d\tilde{\omega} \right) \mathbf{W}(\omega) \mathbf{e} \quad (36)$$

301

302 It can be seen that the calculation of Eq. (36) is only related to $\tilde{\mathbf{G}}(\tilde{\omega})$, which is the Fourier

303 transform matrix of the non-stationary random seismic input modulation function matrix

304 $\mathbf{G}(t)$. The corresponding integral operation is equivalent to the inverse Fourier transform

305 of the kernel function $\mathbf{H}(\tilde{\omega} + \omega) \tilde{\mathbf{G}}(\tilde{\omega})$, but note that the frequency corresponding to the

306 frequency response function is $\tilde{\omega} + \omega$. The modulation function of uniformly modulated

307 non-stationary seismic input is a slowly varying function, so the calculation does not need

308 to use a very high sampling frequency. Also, this analysis process is deterministic, which

309 has a good advantage for ~~fast Fourier transform~~ FFT.

310 Meanwhile, $\boldsymbol{\alpha}_s(t, \omega)$ in Eq. (26) can be rewritten as

311

$$\begin{aligned}\boldsymbol{\alpha}_s(t, \omega) &= \boldsymbol{\beta}_s(t, \omega)\sqrt{S_{\ddot{x}\ddot{x}}(\omega)}e^{i\omega t} \\ \boldsymbol{\beta}_s(t, \omega) &= -\frac{1}{\omega^2}\mathbf{M}_{aa}^{-1}\mathbf{R}\mathbf{G}(t)\mathbf{W}\mathbf{e}\end{aligned}\quad (37)$$

312

313 Substituting Eqs. (35) and (37) into Eq. (30), the evolutionary PSD of the absolute

314 displacement response is given as

315

$$\mathbf{S}_{y_a y_a}(t, \omega) = (\boldsymbol{\beta}_d(t, \omega) + \boldsymbol{\beta}_s(t, \omega))^*(\boldsymbol{\beta}_d(t, \omega) + \boldsymbol{\beta}_s(t, \omega))^T S_{\ddot{x}\ddot{x}}(\omega) \quad (38)$$

316

317 Thus, Eq. (38) gives the semi-analytical solution for the evolutionary PSD of random

318 responses of long-span structures. This solution has a simple form and clear physical

319 interpretations. It indicates that the nonstationary evolutionary PSD of the absolute

320 displacement response is in fact an explicit modulation of the stationary PSD of the

321 ground motion. Hence, when performing the similar nonstationary vibration analysis, it

322 is only necessary to consider the calculation of the deterministic modulation matrix, i.e.

323 $\boldsymbol{\beta}_d(t, \omega)$ and $\boldsymbol{\beta}_s(t, \omega)$ in Eqs. (36) and (37).

324 It should be mentioned that zero initial conditions are used in the above analysis.

325 Compared to conventional time domain methods, the present method is totally

326 implemented in the frequency domain. Since $\boldsymbol{\beta}_d(t, \omega)$ can be calculated by the FFT, a

327 unified approach can be used for different type of modulation functions. Moreover, as

328 well as the displacement calculated above, the evolutionary PSD of other random

329 responses, such as the internal force, can also be solved by the present method without

330 any additional difficulty.

331 **4.3 Evaluation of extreme value response**

332 The evaluation of the peak amplitude responses of long-span structures subjected to
333 nonstationary seismic excitation is a fundamental problem for engineering structural
334 design. In order to evaluate the extreme value responses, the nonstationary random
335 response can be replaced with a stationary one through the energy equivalence over a
336 specific duration T_d .

337 It is assumed that the evolutionary PSD $S_{yy}(t, \omega)$ of any random response $y(t)$
338 of a structure under non-stationary random earthquake is known. Over the duration T_d ,
339 the equivalent stationary PSD $S_{\bar{y}\bar{y}}(\omega)$ can be expressed as [13]

340

$$S_{\bar{y}\bar{y}}(\omega) = \frac{1}{T_d} \int_{t_0/\sqrt{2}}^{t_0/\sqrt{2}+T_d} S_{yy}(t, \omega) dt \quad (39)$$

341

342 From the above equation, the PSD of the equivalent stationary random process $\bar{y}(t)$
343 with the average energy distribution, strong earthquake duration and seismic intensity
344 consistent with the nonstationary stochastic process can be obtained. Denoting the
345 extreme value of $\bar{y}(t)$ within the duration T_d as \bar{y}_e , and the standard deviation as $\sigma_{\bar{y}}$,
346 a dimensionless parameter is defined as

347

$$\eta = \bar{y}_e / \sigma_{\bar{y}} \quad (40)$$

348

349 It is assumed that if a given threshold value is sufficiently high, the peaks of $\bar{y}(t)$

350 above this barrier will appear independently. Then, the number of crossings of the
 351 threshold value will be a Poisson process with a stationary increment [26]. Based on these
 352 assumptions, the probability distribution of η can be derived as

$$P(\eta) = \exp[-vT_d \exp(-\eta^2/2)] \quad (41)$$

354 where
 355
 356

$$v = \sqrt{\lambda_2/\lambda_0}/\pi \quad (42)$$

357
 358 λ_0 and λ_2 are spectral moments of the random process and can be computed by

$$\lambda_k = 2 \int_0^\infty \omega^k S_{\bar{y}\bar{y}}(\omega) d\omega, k = 0, 2 \quad (43)$$

359
 360
 361 Using the probability distribution shown in Eq. (41), the expected value of η is
 362 approximately

$$E(\eta) \approx \sqrt{2 \ln(vT_d)} + \gamma / \sqrt{2 \ln(vT_d)} \quad (44)$$

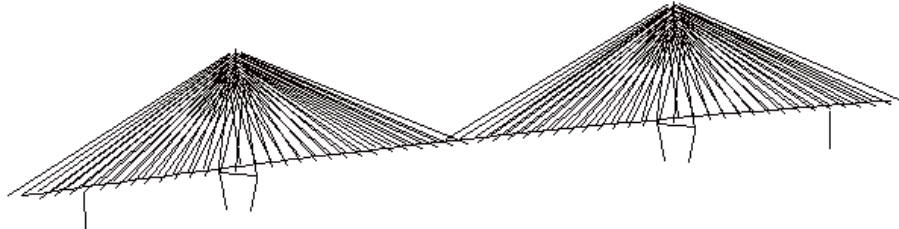
364
 365 in which $\gamma = 0.5772$ is the Euler constant.

366 **5 Numerical examples**

367 The Liaohe bridge lying between Yinkou and Panjin in Liaoning Province, China is
 368 chosen as a numerical example, as shown in Fig. 1. The main structure spanning the Liao
 369 River is a cable-stayed bridge of total length 866m. The finite element model has 429
 370 nodes (including 4 supports), 310 elements and 1156 DOF. The deck and tower are

371 modelled by three dimensional beam elements with stiff arms on both ends and each cable
372 is modelled by one dimensional cable elements.

373

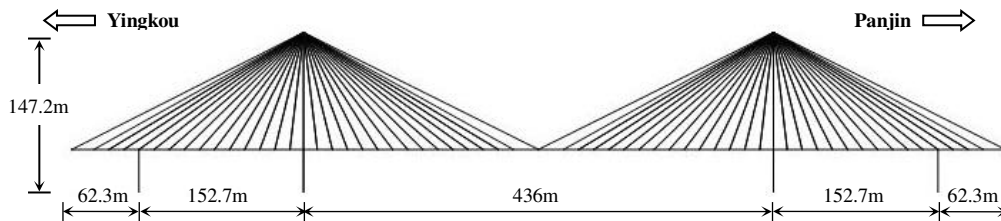


374

(a) Oblique view

375

376



377

378

379

(b) Front view

380

Fig. 1 Schematic of the Liaohe bridge

381

382 The first 200 modes are used in the mode superposition, with the corresponding
383 natural periods ranging within [0.046, 6.135]s. A damping ratio of 0.05 is assumed for all
384 participant modes. The effective frequency region is taken as $\omega \in [0.0, 100]$ rad/s and the
385 frequency step size is $\Delta\omega = 0.2$ rad/s. The ground acceleration response spectrum used
386 is based on the Chinese code (CMC, 2001) [27] with regional fortification intensity 7,
387 site-type 2, and seismic classification 1. The Kaul method [28] is used to generate the
388 ground acceleration PSD compatible with the response spectrum.

389 A uniformly modulated nonstationary seismic excitation model is used here, with

390 the modulation function

391

$$a(t) = \begin{cases} I_0(t/t_1)^2 & 0 \leq t \leq t_1 \\ I_0 & t_1 \leq t \leq t_2 \\ I_0 \exp[c_0(t - t_2)] & t \geq t_2 \end{cases} \quad (45)$$

392

393 where $t_1 = 8.0$ s, $t_2 = 20.0$ s and $c = 0.2$. The duration of the earthquake is $t \in$

394 $[0,60$ s].

395 **5.1 Evolutionary PSD and time-dependent variance**

396 The PEM [24] is used to benchmark the results obtained from the present method.

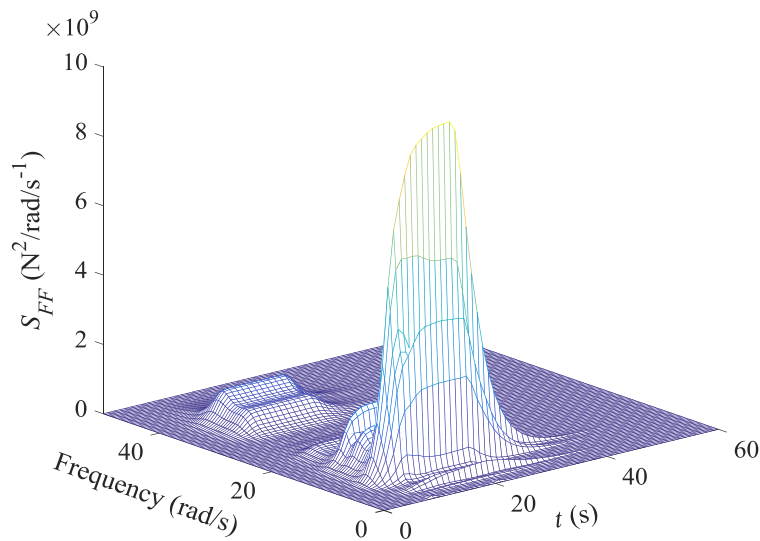
397 The SV waves travelling horizontally along the bridge are considered as the excitation

398 and the wave velocity is $v = 2000$ m/s. A time step with $\Delta t = 0.02$ s is used in the time

399 domain analysis of the PEM, while a sampling frequency $f = 10$ Hz is used in the FFT

400 of the present method. Figs. 2(a) and 2(b) show the evolutionary PSD functions of the

401

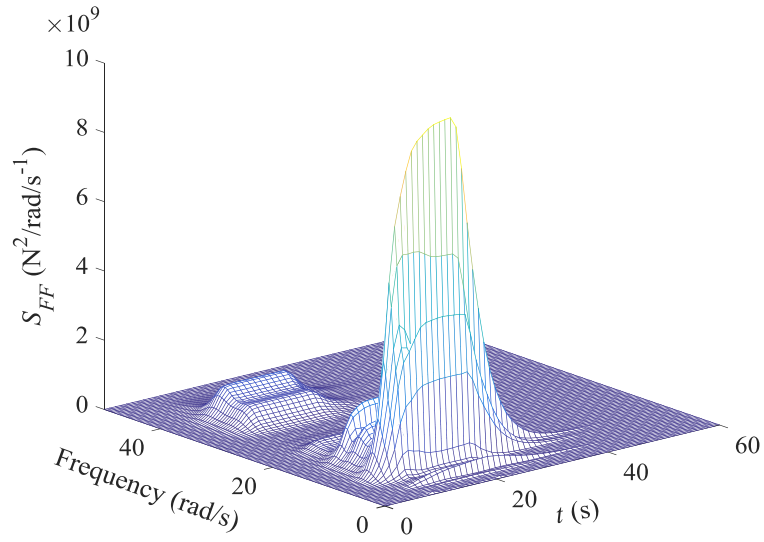


402

403

(a) Results of the PEM

404



405

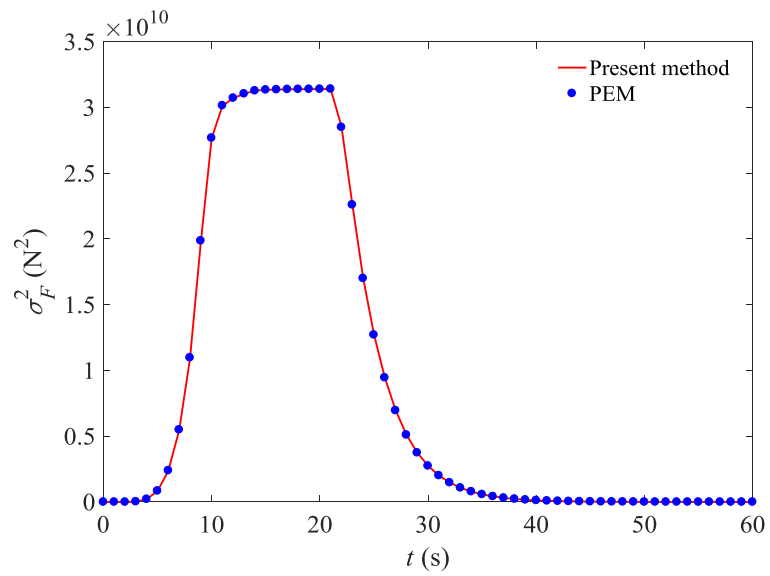
406

(b) Results of the present method

407

Fig. 2 Evolutionary PSD of transverse shear force at the middle of the deck

408



409

410

Fig. 3 Time-dependent variances of transverse shear force at the middle of the deck.

411

412 transverse shear force at the middle of the deck obtained from the PEM and present
 413 method, respectively. It is observed that the results of these two methods agree quite well
 414 and the maximum error is about 0.76%. For further comparison, Fig. 3 gives the time-
 415 dependent variances of the transverse shear force at the middle of the deck. It is seen that
 416 the results obtained by the present method are in excellent agreement with those of the
 417 PEM. The maximum relative error is below 0.4%, and thus the accuracy of the present
 418 method is verified.

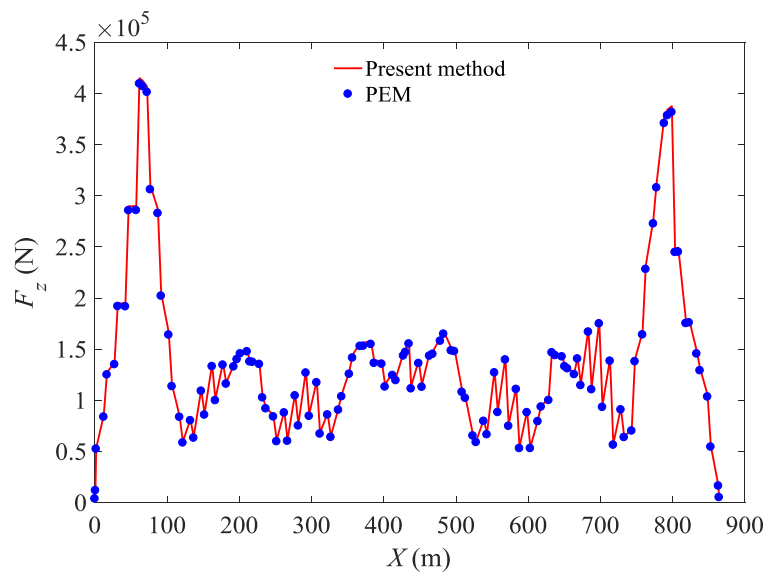
419

420 **5.2 Extreme value response**

421 Considering P waves with wave velocity $v = 1000\text{m/s}$ and SV waves with
 422 $v = 700\text{m/s}$, extreme value responses of the bridge are estimated by the present method
 423 and PEM. Figs. 4(a) and 4(b) present extreme values of the transverse shear forces F_z

424

425

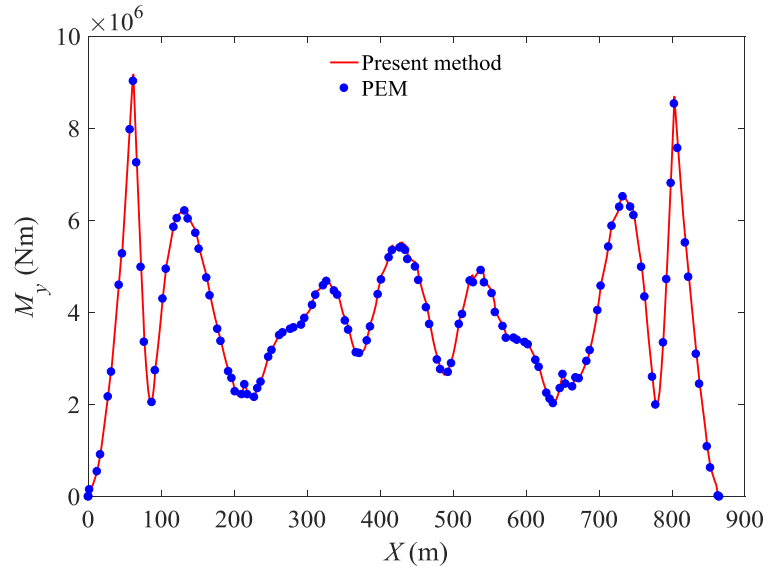


426

427

(a) Transverse shear forces

428



429

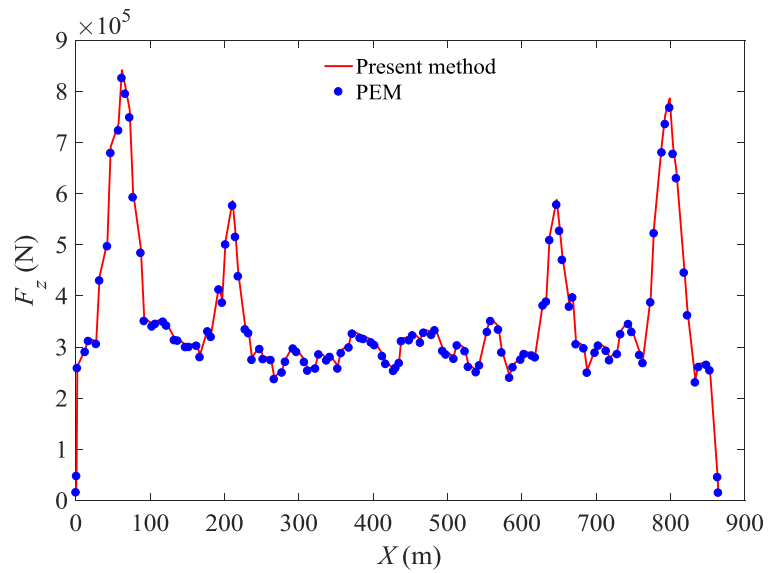
430

(b) Bending moments

431

Fig. 4 Extreme value responses of internal forces under P waves

432

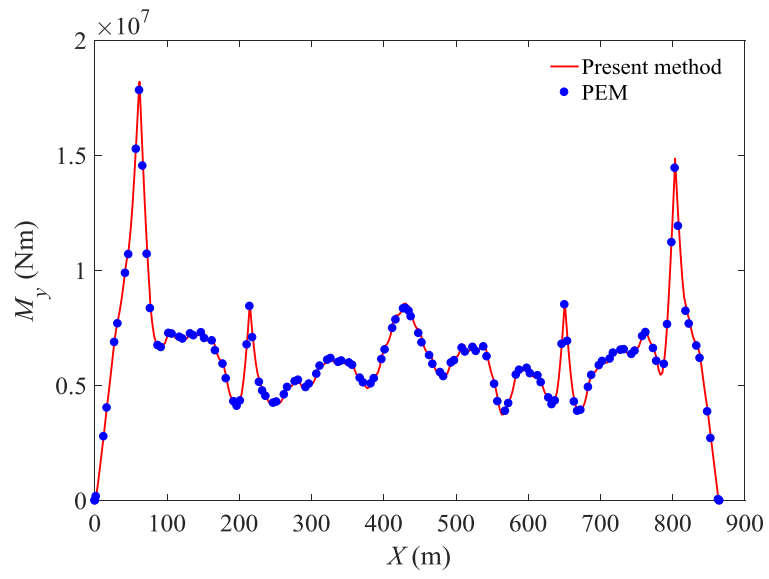


433

434

(a) Transverse shear forces

435



436

437

(b) Bending moments

438

Fig. 5 Extreme value responses of internal forces under SV waves

439

440 and bending moments M_y along the deck under P waves, respectively,
441 while Figs. 5(a) and 5(b) present the same results under SV waves. It is
442 shown that the results using the present method and PEM have a good
443 agreement, demonstrating the accuracy of the present method for extreme
444 value responses. As can be seen from Fig. 4(a), there are two peak values of
445 transverse shear forces at $X = 62\text{m}$ and 803m , i.e. the locations of the left
446 and right bridge piers. This is because the restraints of piers can change the
447 distribution of internal forces and lead to jumps of transverse shear forces.
448 Between these two piers, the distribution of transverse shear forces is
449 comparatively flat. Moreover, due to the symmetry of the bridge and
450 excitation, the overall distribution of transverse shear forces also shows
451 approximate symmetry. Similar phenomena can be observed in Figs. 4(b),
452 5(a) and 5(b), respectively. Computation times of the present method and
453 PEM are 667.52s and 1430.15s, indicating the high efficiency of the present
454 method.

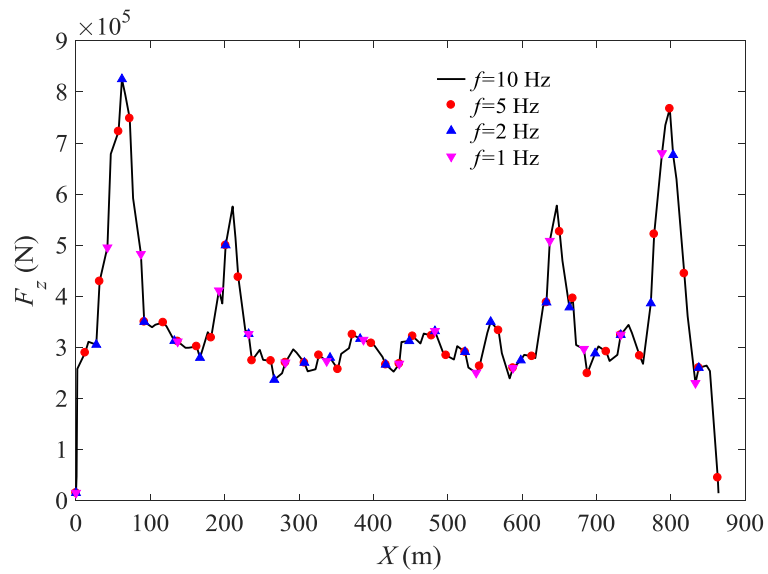
455 **5.3 Performance of the present method with different sampling** 456 **frequencies**

457 In Section 4.2, it was pointed out that for a linear system under uniformly modulated
458 non-stationary random seismic loads, the evolutionary PSD of the response is determined
459 by Eq. (38), and its physical meaning is the evolution modulation of the input stationary

460 stochastic process, which can be determined by the coefficient vectors $\beta_d(t, \omega)$ and
461 $\beta_s(t, \omega)$. For the calculation of $\beta_d(t, \omega)$ by Eq. (36), only the frequency domain
462 transform of the input nonstationary random process modulation is needed. Since slowly
463 varying modulation functions are used to represent the nonstationary characteristic of the
464 ground motion, a small sampling frequency can be used in the FFT to reduce the
465 computational cost. To demonstrate this advantage, the present method is implemented
466 with different sampling frequencies, i.e. $f = 10\text{Hz}$, 5Hz , 2Hz and 1Hz . The extreme
467 transverse shear forces of the bridge under SV waves with $v = 700\text{m/s}$ is shown in Fig.
468 6(a). It is seen that results with different sampling frequencies are almost coincident with
469 each other. For the convenience of comparison, the result with sampling frequency $f =$
470 10Hz is employed as a reference solution, and then relative errors of results with smaller
471 sampling frequencies are given in Fig. 6(b). It can be seen that maximum errors of results
472 with $f = 1\text{Hz}$, 2Hz and 5Hz are respectively 0.2% , 0.05% and 0.025% .

473 Similar to Fig. 6, Fig. 7 shows results for the extreme bending moment with different
474 sampling frequencies. As can be seen from Fig. 7(b), the maximum errors of results with
475 $f = 1\text{Hz}$, 2Hz and 5Hz are respectively 0.25% , 0.1% and 0.025% . The computation
476 times corresponding to different sampling frequencies are shown in Table 1. It is observed
477 that the computation time for $f = 1\text{Hz}$ is 284.18s , which is about 40% of that for $f =$
478 10Hz . Thus, from the results above, it appears that the present method can be
479 implemented with a very small sampling frequency while retaining very high accuracy,

480 and hence its computational efficiency is improved significantly.

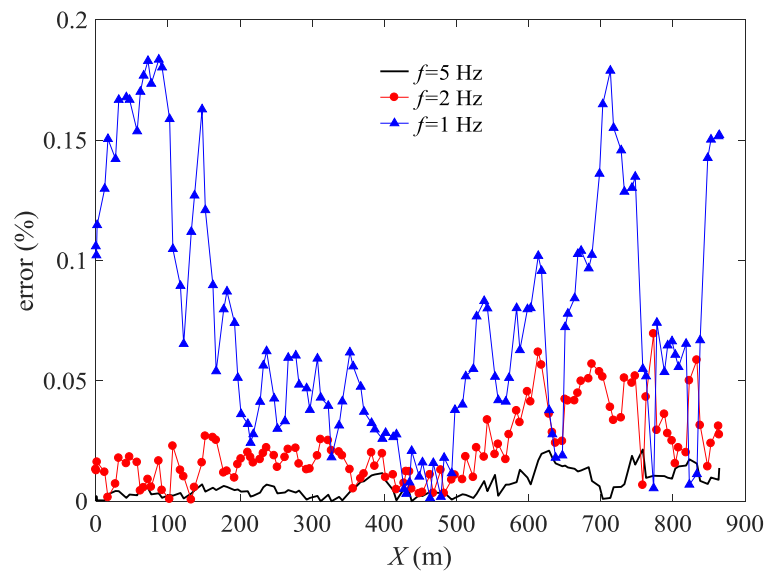


481

482

(a) Transverse shear forces

483



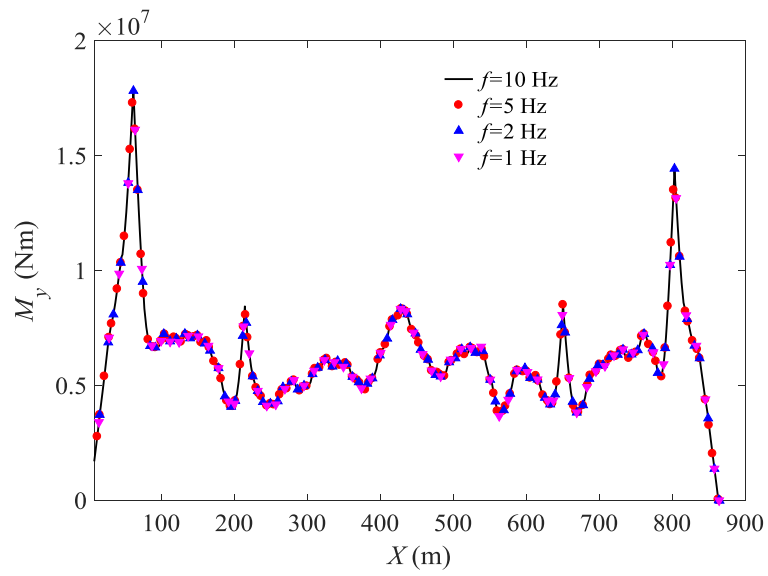
484

485

(b) Relative error

486 Fig. 6 Extreme value transverse shear forces with different sampling frequencies

487

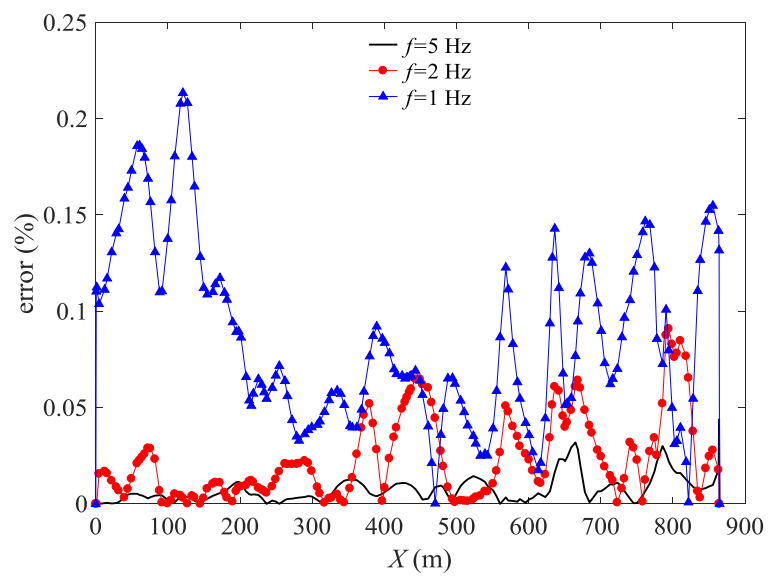


488

489

490

(a) Bending moment



491

492

(b) Relative error

493 Fig. 7 Extreme value bending moments with different sampling frequencies

494

495

496 Table 1 Computation times of the present method with different sampling frequencies

Sampling frequencies (Hz)	10	5	2	1
Time (s)	667.52	311.65	305.69	284.18

497

498 **5.4 Influences of the wave passage effect on responses**

499 Influences of the wave passage effect on random seismic responses are investigated.

500 ~~Consider the response of the structure under SV waves propagating along the longitudinal~~

501 ~~direction of the bridge with velocities $v = 600\text{m/s}$, 650m/s , 700m/s and 750m/s . The~~

502 ~~modal number, frequency domain analysis parameters and nonstationary seismic models~~

503 ~~are the same as above.~~ SV waves propagating along the longitudinal direction of the

504 bridge with velocities $v = 600\text{m/s}$, 650m/s , 700m/s and 750m/s are considered for the

505 seismic response of the bridge, while the modal number, frequency domain analysis

506 parameters and nonstationary seismic models are the same as above. The frequency

507 domain analysis method proposed in this paper is used with sampling frequency $f =$

508 2Hz. Fig. 8(a) gives transverse shear forces with different wave velocities. It is observed

509 that, as the wave velocity increases, these differ slightly outside the two side piers, i.e. in

510 the ranges 0 to 62.3m and 803.7 to 866m, but differ significantly between these two piers,

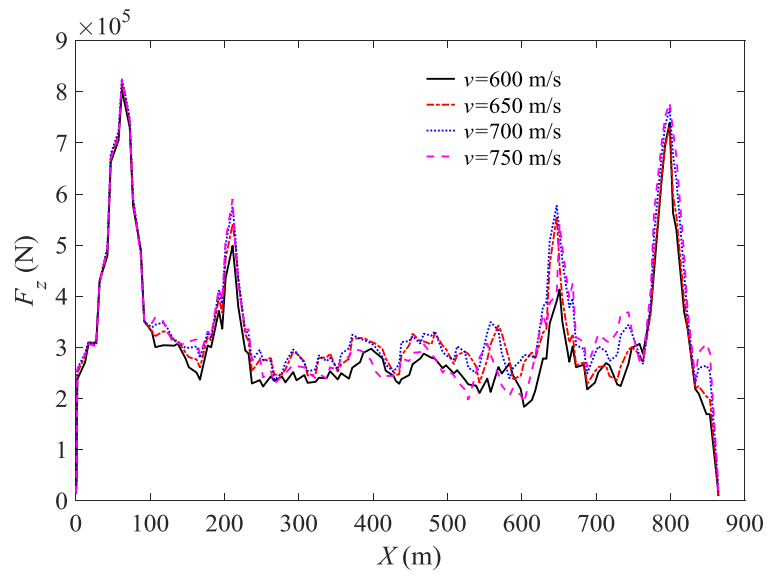
511 i.e. in the range 62.3 to 803.7m.

512 According to random vibration analysis of the structure under multi-input

513 nonstationary seismic excitation in Section 4, the absolute displacement response of the

514 structure is generated by the dynamic relative displacement response and the quasi-static
515 displacement response. In fact, the long-span cable-stayed bridge can be regarded as a
516 complex floating system, and the force transmission path is the main deck drawn by the
517 cable, and passed to the bridge tower, and then passed to the foundation. At the same time
518 the deck also is restrained by the two side piers. Considering the wave effect of seismic
519 propagation, the quasi-static displacement caused by the non-uniform motion of the
520 supports has a significantly higher effect on the shear force of the deck between the two
521 side piers. Fig. 8 (b) shows the results of the calculation of the bending moment of the
522 main deck under different wave velocities. Similar phenomena are observed to those of
523 the shear response. In addition, it can be seen from Figs. 8 (a) and 8 (b) that there is no
524 obvious law for the variation of the peak value of the response, which is influenced by
525 the quasi-static displacement response and the dynamic relative displacement response.
526 For a complex structure, it is often difficult to determine which type of vibration mode
527 has a major effect on its seismic response, and the apparent wave velocity obtained under
528 different earthquakes is often very different. In engineering practice, in the absence of
529 sufficiently reliable wave velocity measurement data, it is appropriate to select the most
530 unfavorable situation as a design basis.

531

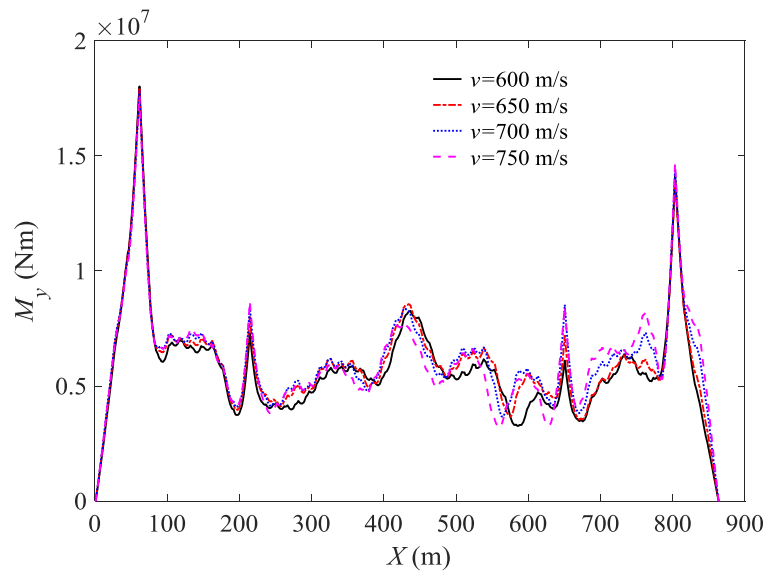


532

533

534

(a) Transverse shear forces



535

536

(b) Bending moments

537

Fig. 8 Internal forces with different wave velocities

538

539

540 **6 Conclusions**

541 This paper presents a frequency domain method for the seismic response analysis of
542 long-span structures subjected to nonstationary random ground motions with
543 consideration of the wave passage effect. A semi-analytical solution is derived for the
544 evolutionary PSD of the response. The following conclusions can be drawn:

545 (1) The nonstationary evolutionary PSD of responses can be represented explicitly
546 as the modulation of the stationary PSD of the ground motion, while the corresponding
547 modulation matrix can be obtained from the nonstationary modulation function. For
548 slowly varying modulation functions, a small sampling frequency can be used in the FFT
549 and hence the present method gains its high efficiency.

550 (2) The results presented for a cable-stayed bridge show that the wave passage effect
551 has significant influence on the random response and hence should be considered in the
552 seismic analysis of long-span structures. The actual seismic response is determined by
553 the dynamic relative displacement and the quasi-static displacement. When seismic
554 analysis is carried out for a multiply supported structure, the influence of the wave
555 passage effect should be taken into account.

556 (3) Since the wave passage effect of ground motions is considered, supports of long-
557 span structures will motion in different phases, which may result two further effects, i.e.,
558 the non-uniform dynamic subsidence of supports and the cancellation of inertia forces.
559 These two effects have opposing influences on dynamic responses of long-span structures.

560 Hence, it is possible for the responses to be larger or smaller after considering the wave
561 passage effect, and these changes cannot be determined a priori. In practical engineering,
562 in the absence of sufficiently reliable wave velocity measurement data, it is recommended
563 to perform a series of seismic analyses with different wave velocities and then select the
564 most unfavorable situation as a basis for design.

565

566 **Acknowledgments**

567 The authors are grateful for support under grants 11772084 and 11672060 from the
568 National Science Foundation of China, and from the Cardiff University Advanced
569 Chinese Engineering Centre.

570

571 **References**

- 572 [1] Loh CH, Yeh YT. Spatial variation and stochastic modelling of seismic differential
573 ground movement. *Earthq Eng Struct Dyn* 1988; 16(4): 583-596.
- 574 [2] Zerva A. Effect of spatial variability and propagation of seismic ground motions on
575 the response of multiply supported structures. *Probabilist Eng Mech* 1991; 6(3-4):
576 212-221.
- 577 [3] Werner SD, Lee LC, Wong HL. Structural response of traveling seismic waves.
578 *ASCE J Struct Div* 1979; 105(12): 2547-2564.
- 579 [4] Der Kiureghian A, Neuenhofer A. Response spectrum method for multi-support

- 580 seismic excitations. *Earthq Eng Struct Dyn* 1992; 21(8): 713-740.
- 581 [5] Yamamura N, Tanaka N. Response analysis of flexible MDF systems for multiple-
582 support seismic excitations. *Earthq Eng Struct Dyn* 1990; 19(3): 345-357.
- 583 [6] Berrah M, Kausel E. Response spectrum analysis of structures subjected to spatially
584 varying motions. *Earthq Eng Struct Dyn* 1992; 21(6): 461-470.
- 585 [7] Heredia-Zavoni E, Vanmarcke EH. Seismic random-vibration analysis of
586 multisupport-structural systems. *J Eng Mech* 1994; 120(5): 1107-1128.
- 587 [8] Lee MC, Penzien J. Stochastic analysis of structures and piping systems subjected to
588 stationary multiple support excitations. *Earthq Eng Struct Dyn* 1983; 11(1): 91-110.
- 589 [9] Lin YK, Zhang R, Yong Y. Multiply supported pipeline under seismic wave
590 excitations. *J Eng Mech* 1990; 116(5): 1094-1108.
- 591 [10]Zanardo G, Hao H, Modena C. Seismic response of multi-span simply supported
592 bridges to a spatially varying earthquake ground motion. *Earthq Eng Struct Dyn* 2002;
593 31(6): 1325-1345.
- 594 [11]Tubino F, Carassale L, Solari G. Seismic response of multi-supported structures by
595 proper orthogonal decomposition. *Earthq Eng Struct Dyn* 2003; 32(11): 1639-1654.
- 596 [12]Lupoi A, Franchin P, Pinto PE, Monti G. Seismic design of bridges accounting for
597 spatial variability of ground motion. *Earthq Eng Struct Dyn* 2005; 34(4-5): 327-348.
- 598 [13]Lin JH, Zhang YH, Zhao Y, “Seismic random response analysis”, in *Bridge*
599 *Engineering Handbook*, W.F. Chen and L. Duan, Eds, Boca Raton 2014; 133-162.

- 600 [14]Zhang YH, Li QS, Lin JH, Williams FW. Random vibration analysis of long-span
601 structures subjected to spatially varying ground motions. *Soil Dyn Earthq Eng* 2009;
602 29(4): 620-629
- 603 [15]Flandrin P, Martin W. “The Wigner-Ville spectrum of nonstationary random signals”
604 in *The Wigner Distribution-Theory and Applications in Signal Processing*,
605 Mecklenbräuker W and Hlawatsch F, Eds. Amsterdam, the Netherlands: Elsevier
606 1997; 211-267.
- 607 [16]Mark WD. Spectral analysis of the convolution and filtering of non-stationary
608 stochastic processes. *J Sound Vib* 1970; 11(1): 19-63.
- 609 [17]Priestley MB, Evolutionary spectra and non-stationary processes, *J Roy Stat Soc Ser*
610 *B-Stat Methodol* 1965; 27(2): 204-237.
- 611 [18]Priestley MB. Power spectral analysis of non-stationary random processes. *J Sound*
612 *Vib* 1967; 6(1): 86-97.
- 613 [19]Jin XL, Huang ZL, Leung AYT. Nonstationary seismic responses of structure with
614 nonlinear stiffness subject to modulated Kanai-Tajimi excitation. *Earthq Eng Struct*
615 *Dyn* 2012; 41(2): 197-210.
- 616 [20]Peng BF, Conte JP. Closed-form solutions for the response of linear systems to fully
617 nonstationary earthquake excitation. *J Eng Mech* 1998; 124(6): 684-694.
- 618 [21]Deodatis, G. Non-stationary stochastic vector processes: seismic ground motion
619 applications. *Probabilist Eng Mech* 1996; 11(3): 149-167.

- 620 [22]Alderucci T, Muscolino G. Fully nonstationary analysis of linear structural systems
621 subjected to multicorrelated stochastic excitations. ASCE-ASME J Risk Uncertainty
622 Eng Syst, Part A: Civ Eng 2016; 2(2): C4015007.
- 623 [23]Ozer E, Feng MQ, Soyoz S. SHM-integrated bridge reliability estimation using
624 multivariate stochastic processes. Earthq Eng Struct Dyn 2015; 44(4): 601-618.
- 625 [24]Lin JH, Zhao Y, Zhang YH. Accurate and highly efficient algorithms for structural
626 stationary/non-stationary random responses. Comput Methods Appl Mech Eng 2001;
627 191(1-2): 103-111.
- 628 [25]Clough RW, Penzien J. Dynamics of Structures. New York: McGraw-Hill; 1993.
- 629 [26]Davenport AG. Note on the distribution of the largest value of a random function
630 with application to gust loading. Proc Inst Civil Eng 1964; 28(2): 187-196.
- 631 [27]China Ministry of Construction. Code for seismic design of buildings GB 50011-
632 2001. Beijing: Chinese Architectural Industry Press; 2001 (in Chinese).
- 633 [28]Kaul MK, Stochastic characterization of earthquakes through their response
634 spectrum. Earthq Eng Struct Dyn 1978; 6(5): 497-510.